

GENETIC AND MOLECULAR DISSECTION OF RHABDOMYOSARCOMA  
TUMORIGENESIS

APPROVED BY SUPERVISORY COMMITTEE

Committee Chairperson's Name: Rene Galindo, M.D., Ph.D.

Committee Member's Name: Diego Castrillon, M.D., Ph.D.

Committee Member's Name: Mark Hatley, M.D., Ph.D.

GENETIC AND MOLECULAR DISSECTION OF RHABDOMYOSARCOMA  
TUMORIGENESIS

by

LAUREN A. EDELMAN

DISSERTATION

Presented to the Faculty of the Medical School

The University of Texas Southwestern Medical Center at Dallas

In Partial Fulfillment of the Requirements

For the Degree of

DOCTOR OF MEDICINE WITH DISTINCTION IN RESEARCH

The University of Texas Southwestern Medical Center at Dallas

Dallas, Texas

August, 2011

## ABSTRACT

### MOLECULAR DISSECTION OF RHABDOMYOSARCOMA TUMORIGENESIS

LAUREN A. EDELMAN

The University of Texas Southwestern Medical Center at Dallas, 2011

Supervising Professor: Rene Galindo

Rhabdomyosarcoma is a tumor of skeletal muscle-type histogenesis and the most common pediatric soft tissue cancer. Rhabdomyosarcoma is often caused by one of two chromosomal translocations,  $t(1;32)(q35;q14)$  or  $t(2;13)(p36;q14)$ , that are rhabdomyosarcoma - specific and diagnostic, and both drive equivalent PAX-FKHR fusion oncogenic transcription factors. Despite aggressive multimodal therapy, the 5-year survival rate of patients with advance-staged rhabdomyosarcoma remains less than 30% and has not improved in three decades. We intend to genetically characterize the molecular underpinnings of rhabdomyosarcoma to find new potential drug targets for treatment. Since PAX biology is structurally and functionally conserved (as is syncytial muscle development and structure), we have generated a new transgenic *PAX-FKHR Drosophila* model, which we have used to conduct a forward unbiased genetic screen to identify dominant modifiers of PAX-FKHR pathogenesis when expressed in growing muscle tissue. We also performed microarray analysis of fly *PAX-FKHR* tissue versus

control tissue. We are now actively profiling genetic loci of interest for phenotypes in mammalian murine C2C12 myoblasts. After testing a subset of candidate genes identified in the screen, we have found that the genes identified as genetic modifiers of PAX-FKHR pathogenicity in the fly screen are indeed active in mammalian myoblast biology and PAX-FKHR pathobiology. These genes include loci normally involved in myogenesis and genes not previously correlated with mammalian skeletal muscle development or PAX biology. Our results suggest that the *PAX-FKHR Drosophila* transgenic model and genetic screening are revealing previously unknown gene targets that will likely underlie rhabdomyosarcoma pathogenesis. The discovery of new genes seminal to rhabdomyosarcoma pathobiology will be a valuable tool in the conceptual design of new therapies to target rhabdomyosarcoma and thus improve treatment.

## TABLE OF CONTENTS

PRIOR PUBLICATIONS AND PRESENTATIONS .....	7
LIST OF FIGURES.....	8
CHAPTER ONE—RHABDOMYOSARCOMA .....	9
CHAPTER TWO—ANIMAL MODELS OF PAX-FKHR RHABDOMYOSARCOMA .	12
CHAPTER THREE—MECHANISMS OF PAX-FKHR RHABDOMYOSARCOMA ....	28
BIBLIOGRAPHY .....	39
VITAE .....	41

## PRIOR PUBLICATIONS AND PRESENTATIONS

Edelman LA, Mummert ME. 2009. Detection of Hyaluronidase Activity In Vitro Using

FRET-HA. *47th Medical Student Research Forum Booklet*. 13.

Edelman LA, Galindo RL. 2010. Molecular Dissection of Rhabdomyosarcoma

Tumorigenesis. *48<sup>th</sup> Medical Student Research Forum Booklet*. 6.

Edelman LA, Avirneni-Vadlamudi U, Tran LT, Galindo, RL. 2010. Molecular Dissection of Rhabdomyosarcoma Tumorigenesis. *Journal of Investigative Medicine*. 58:453.

Lauren A. Edelman, Oral Presentation, **Southern Regional Meeting**, New Orleans, LA, 2010.

## LIST OF FIGURES

FIGURE ONE— STRUCTURE OF PAX3/7 GENE AND FKHR FUSION GENE .....	11
FIGURE TWO— PAX3/7 IS CONSERVED IN DROSOPHILA .....	18
FIGURE THREE—FKHR EXPRESSION CAUSES MUSCLE FIBER DISARRAY. ....	20
FIGURE FOUR— PAX7-FKHR CAUSES MONONUCLEAR CELL DEVELOPMENT	22
FIGURE FIVE—PAX7-FKHR CELLS INFILTRATE THE LARVAL CNS.....	23
FIGURE SIX— ACTIVATED RAS ENHANCES PAX7-FKHR ACTIVITY.....	24
FIGURE SEVEN— LOSS-OF-FUNCTION RAS SUPPRESSES PAX7-FKHR .....	25
FIGURE EIGHT— LOSS OF M-ANTS1 BLOCKS FORMATION OF MYOTUBES.....	32
FIGURE NINE— M-ANTS1-SILENCED CELLS SHOW SIMILAR LEVELS OF MHC	33
FIGURE TEN— SILENCING M-ANTS1 DRAMATICALLY ALTERS PHENOTYPE.	35
FIGURE ELEVEN— SILENCING H-ANTS1 SHOWS PARTIAL RESCUE .....	36

# **CHAPTER ONE**

## **Introduction**

### **RHABDOMYOSARCOMA**

Rhabdomyosarcoma, in the family of cancers of the musculoskeletal system, is the most common soft tissue cancer among children under 15 years of age and accounts for approximately half of childhood soft tissue cancers [1]. The incidence is roughly 4 – 7 cases per million children in the USA which corresponds to 350 new cases annually [2]. While it can present anywhere, it most often occurs in extremities, genitourinary system, and head and neck region. Because treatment often involves invasive surgical removal, chemotherapy, and radiation, even those cured of rhabdomyosarcoma often face lifelong deformities particularly with rhabdomyosarcoma in the head and neck [1]. In spite of advances in chemotherapy and aggressive multimodal therapy, the 5-year survival rate of patients with advance-staged rhabdomyosarcoma remains at less than 30 % and has not improved in over three decades [3].

Rhabdomyosarcoma can be divided into two major subtypes based on histology: alveolar rhabdomyosarcoma and embryonal rhabdomyosarcoma [4]. These two subtypes are both genetically and histologically distinct, which is clinically relevant because alveolar rhabdomyosarcoma is an independent predictor of worse outcome and associated with more frequent occurrence of metastasis at the time of initial diagnosis [3]. There is regional lymphatic spread in roughly half of the cases of alveolar rhabdomyosarcoma at diagnosis [1]. Not only does alveolar rhabdomyosarcoma show more aggressive behavior, but it also exhibits diminished response to current therapies as compared with embryonal rhabdomyosarcoma [2]. Histologically, it is characterized by the presence of

8



primitive tumor cells lining fibrovascular septa, which form alveolar-like spaces containing round, malignant cells with characteristic eosinophilic cytoplasm [5]. Embryonal rhabdomyosarcoma comprises 50 to 60 percent of all cases of rhabdomyosarcoma, but the prognosis for embryonal rhabdomyosarcoma is significantly better than for alveolar rhabdomyosarcoma with a five-year survival rate of 88 percent [5]. It is histologically distinguished by varying numbers of spindle and primitive round cells in a myxoid background with characteristic rhabdomyoblasts that are eosinophilic, unusually shaped, and often contain distinctive cross striations [5].

The pathogenesis of alveolar rhabdomyosarcoma differs from embryonal rhabdomyosarcoma because unlike the embryonal variant, alveolar rhabdomyosarcoma is associated with chromosomal translocations [1]. Alveolar rhabdomyosarcoma is linked with acquired alveolar rhabdomyosarcoma-specific chromosomal translocations of  $t(1;32)(q35;q14)$  or  $t(2;13)(p36;q14)$  in 70 to 85 percent of cases [4]. This leads to the fusion of the PAX3 or PAX7 transcription factor to the forkhead in human rhabdomyosarcoma (FKHR) transcription factor (Fig. 1). All characterized PAX-FKHR chromosomal translocations produce structurally equivalent, in-frame PAX-FKHR chimeric transcription factors, where the PAX paired box and homeodomain DNA-binding domains are fused to the transcriptional activation domain of FKHR. The effect of these translocations is the misexpression of the PAX-FKHR oncoprotein, and because both PAX3 and PAX7 are transcription factors that play a role in skeletal muscle development, it is thought to misregulate aspects of the muscle development, growth and/or maintenance. This drives neoplastic transformation of skeletal muscle lineage tissues towards malignant, developmentally arrested primitive myoblast [6].

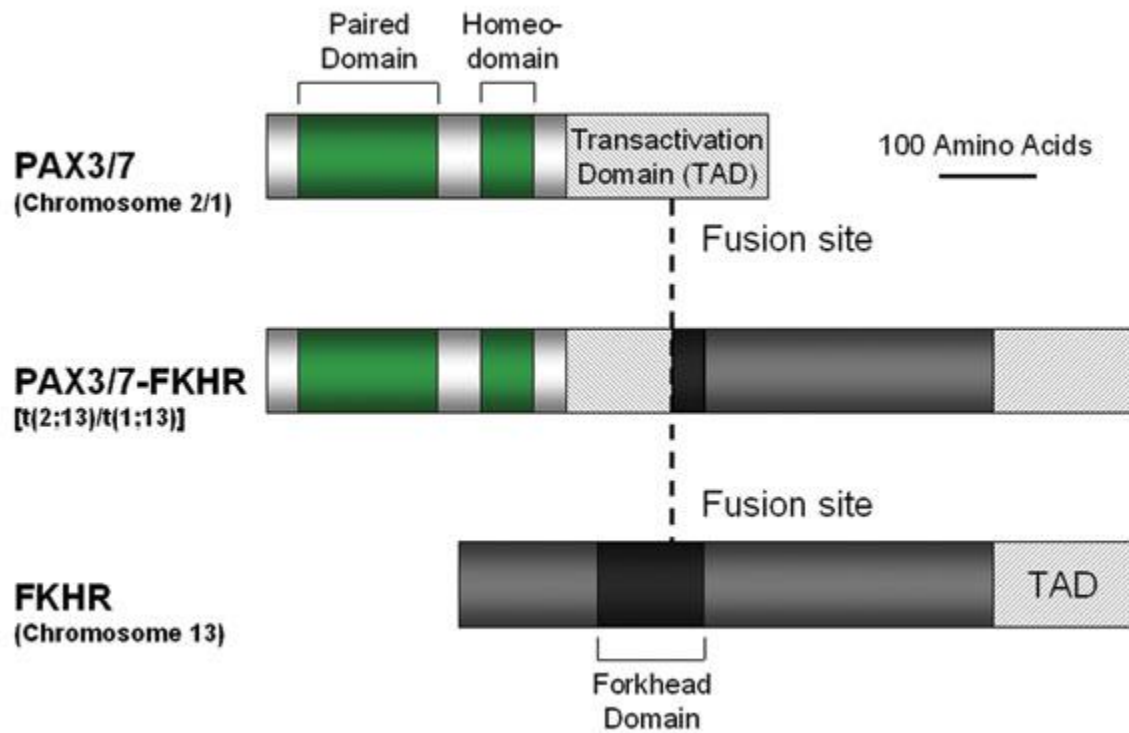


**Fig. 1.** The structure of the PAX3/7 gene (the PAX3 gene is on chromosome 2 and the PAX7 gene is on chromosome 1), the forkhead in human rhabdomyosarcoma (FKHR) gene on chromosome 13, and the chimeric PAX-FKHR product produced by the fusion of the two genes which is seen in the translocations commonly found in alveolar rhabdomyosarcoma. The fusion point is represented by the dashed line. Because all characterized alveolar rhabdomyosarcoma translocations occur within the same PAX3/7 and FKHR introns, the resulting oncoproteins have identical structures [6].

## **CHAPTER TWO**

### **Animal Models of PAX-FKHR Rhabdomyosarcoma**

#### **BACKGROUND**

In order to understand the role of the PAX3-FKHR oncoprotein in the tumorigenesis of alveolar rhabdomyosarcoma, a PAX3-FKHR expressing transgenic mouse model was developed [7]. PAX3 and PAX7 are important transcription regulatory factors in neural tube and myogenic development during embryogenesis [8]. PAX3 defective mice fail to form normal embryonic muscles whereas PAX7 defective mice have impaired formation of satellite cell derived postnatal muscles which comprise a considerable amount of adult muscle mass. Murine models with prenatal expression of PAX3-FKHR display severe birth defects including cranioschisis, exencephaly, and characteristic skeletal dysplasias that show normally organized but hypoplastic limb muscles. This suggests that the chromosomal translocation that results in the PAX3/7-FKHR oncoprotein seen in human alveolar rhabdomyosarcoma does not occur by way of germ line mutations [7]. In fact, the activation of PAX3-FKHR expression in somite-derived myogenic precursors, embryonic satellite cells, and postnatal satellite cell pools does not produce or initiate alveolar rhabdomyosarcoma tumorigenesis in the murine models [3].

In the mouse PAX-FKHR study, Keller et al. used a transgenic mouse which contained a PAX3-FKHR knock-in allele that can be triggered in distinct tissue-specific lineages via breeding with muscle-specific Cre drivers. The Pax3-Fkhr knock-in allele allows normal expression of Pax3 and Fkhr genes, so the animals are *wild-type* until Cre

is present, at which point it is converted into a Pax3-Fkhr allele. After 12 months, one in 228 mice heterozygous for the Pax3-Fkhr allele demonstrated the presence of a tumor derived from a Cre-expressing cell, which was consistent with alveolar rhabdomyosarcoma both histologically and immunohistochemically [3].

Because disruption of Ink4a/ARF and Trp53 pathways has been found in specimens of human alveolar rhabdomyosarcoma, they then introduced conditional inactivation of the Ink4a/ARF or Trp53 pathways in the target pool of terminally differentiating skeletal muscle to determine whether these additional mutations would accelerate alveolar rhabdomyosarcoma development. After breeding for homozygosity of these mutations, two of five mice with Trp53 mutations, and four of 14 mice with Ink4a/ARF mutations showed evidence of tumor formation by age 3 months. Like the previous PAX3-FKHR expressing model, these tumors were determined to be classic alveolar rhabdomyosarcoma by both histology and immunohistochemistry [3].

These PAX3-FKHR murine models are useful to elucidate potential pathways for tumorigenesis as well as potential cells of origin for alveolar rhabdomyosarcoma. Frequently, pediatric cancers are associated with chromosomal translocations which are often asymptomatic at birth [9]. Because the mouse models expressing PAX3-FKHR prenatally show such severe birth defects and lethality, it is unlikely that these translocation events occur as germ-line mutations or as a mosaic affecting a broad range of myogenic precursors. The murine models suggest that postnatal, terminally differentiating myofibers are capable of and thus presumably underlies most alveolar rhabdomyosarcomas. The loss of replicative checkpoints would be advantageous for the expansion of myogenic precursors or satellite cells transforming into rhabdomyosarcoma,

but would be critical for rhabdomyosarcoma resulting from transformation of terminally differentiating myofibers in quiescence [3]. This is consistent with the fact that roughly 40 % of human rhabdomyosarcomas show evidence of absent or aberrant Trp53 [10].

The tumors produced by the animal models have similar immunohistochemical profiles to human alveolar rhabdomyosarcomas including marked derangement of the expression of early myogenic markers and markers of proliferation [3]. The ability of the mouse models to generate similar tumors to human alveolar rhabdomyosarcoma suggests it could be valuable for preclinical therapeutic testing [4]. Unfortunately, because of technical limitations of the model itself, more in depth genetic dissection of these tumors as well as capturing the cells originating from differentiated skeletal muscle were unable to be done. This leaves room for speculation regarding the mechanisms of pathogenesis, level of development of the cells involved in tumorigenesis, and prevents further investigation of alveolar rhabdomyosarcoma biology [6].

In order to further study the consequences of PAX-FKHR expression in differentiated muscle, we generated transgenic fruit flies expressing human PAX-FKHR in somatic muscle. Utilizing *Drosophila melanogaster* allows us to take advantage of the fact that the entire somatic musculature of the animal, when expressing fluorescent protein reporters, is easily visualized through the transparent outer cuticle, and allows us to detect muscle abnormalities induced by PAX-FKHR, even if subtle or focal. This particular animal model is also sensitive to both genetic suppression and enhancement, which will allow us to characterize the pathogenetic mechanisms underlying tumorigenesis. Furthermore, this PAX-FKHR model is conducive to unbiased genetic screens which have the potential to reveal previously unknown PAX-FKHR gene targets

and cofactors that are useful starting points for the conceptual development of therapeutics.

## **METHODS**

The pUAST [11] constructs were generated as follows: (i) UAS-PAX7-FKHR cDNA (100 bp of 5' UTR, 2,490 bp of coding sequence, and 1,180 bp of 3' UTR) was cloned by flanking NotI (5') and XbaI (3') cleavage sites; (ii) UAS-PAX3-FKHR cDNA (24 bp of 5' UTR, 2,508 bp of coding sequence, and 1,178 bp of 3' UTR) was cloned by flanking BgIII (5') and XbaI (3') cleavage sites; and (iii) UAS-PAX3-cDNA (24 bp of 5' UTR, 1,437 bp of coding sequence, and 173 bp of 3' UTR) was cloned by flanking EcoRI (5') and XbaI (3') cleavage sites.

We generated UAS-PAX7-FKHR, UAS-PAX3-FKHR, and UAS-PAX3 transgenic lines by P-element-mediated gene transfer. The remaining stocks were UAS-2xeGFP-AH2, UAS-Ras85D.V12-TL1, Ras85De2F, Ras85De1B, and Myosin heavy chain-Gal4.

For the lethal-phase test study, conducted at 29°C, control (wild type) or PAX7-FKHR virgin females were mated to MHC-Gal4 males. Genotypes were as follows: wild type = w<sup>1118</sup>;+; +; PAX7-FKHR<sup>-2</sup> = w<sup>1118</sup>;UAS-PAX7-FKHR<sup>-2</sup>;+; +; PAX7-FKHR<sup>-3D</sup> = w<sup>1118</sup>;UAS-PAX7-FKHR<sup>-3D</sup>; +; and MHC-Gal4 = w<sup>1118</sup>;UAS-2xeGFP;MHC-Gal4. Fertilized embryos were allowed to hatch on wet yeasted apple juice plates, with the animals transferred as first-instar larvae to prewarmed dry yeasted cornmeal agar vials. Dead larvae were staged as second or third instars by their anterior spiracles (41). The number of animals not scored represents animals injured or lost during the course of the study.

For the time-course study, newly hatched (day 0) UAS-PAX7-FKHR -2;UAS-2xeGFP-AH2;MHC-Gal4 larvae were obtained and individually placed into separate, wet yeasted grape juice plates and raised at 25°C or 29°C. The animals were examined daily for the next 4 days. When necessary, larvae were placed at -20°C for ≈5 min to temporarily immobilize the animals for photographic purposes.

To prepare *Drosophila* larvae for histologic processing, the anterior-most and/or posterior-most aspect of the larval cuticle was breached with a razor blade to facilitate formalin penetration and fixation of internal tissue. The fixed tissue was then processed for routine histology and embedded in paraffin. Sections were cut at 3 μm and stained with hematoxylin and eosin.

## **RESULTS**

In order to investigate the role of misexpression of PAX-FKHR in the biology of differentiated skeletal muscle, we conditionally expressed PAX-FKHR in *Drosophila* via the bipartite Gal4-UAS expression system [11]. By crossing so that genomic enhancers regulate Gal4 expression temporally and spatially, we generated sets of *UAS-PAX3-FKHR* and *UAS-PAX7-FKHR* transgenic *Drosophila* lines that incorporate human *PAX-FKHR* cDNA. UAS-transgene expression occurs in strict tissue-specific patterns.

We hypothesized this would provide a valid model for examining PAX-FKHR muscle biology for several reasons. The functional DNA-binding motifs in the PAX-FKHR oncoprotein are derived from the PAX portion of the fusion protein (Fig. 1). The *PAX3/7* genes are conserved in *Drosophila*, represented by the *gooseberry* (*gsb*) and



*gooseberry-neuro* (*gsb-n*) genes (Fig. 2), and similar to mammalian PAX3/7 both *gsb* and *gsb-n* are expressed in embryonic ectodermal and mesodermal tissues [12]. Also notable is the fact that mammalian PAX3 can functionally substitute for *Drosophila* PAX [13], showing that PAX3/7 are functionally and structurally conserved.

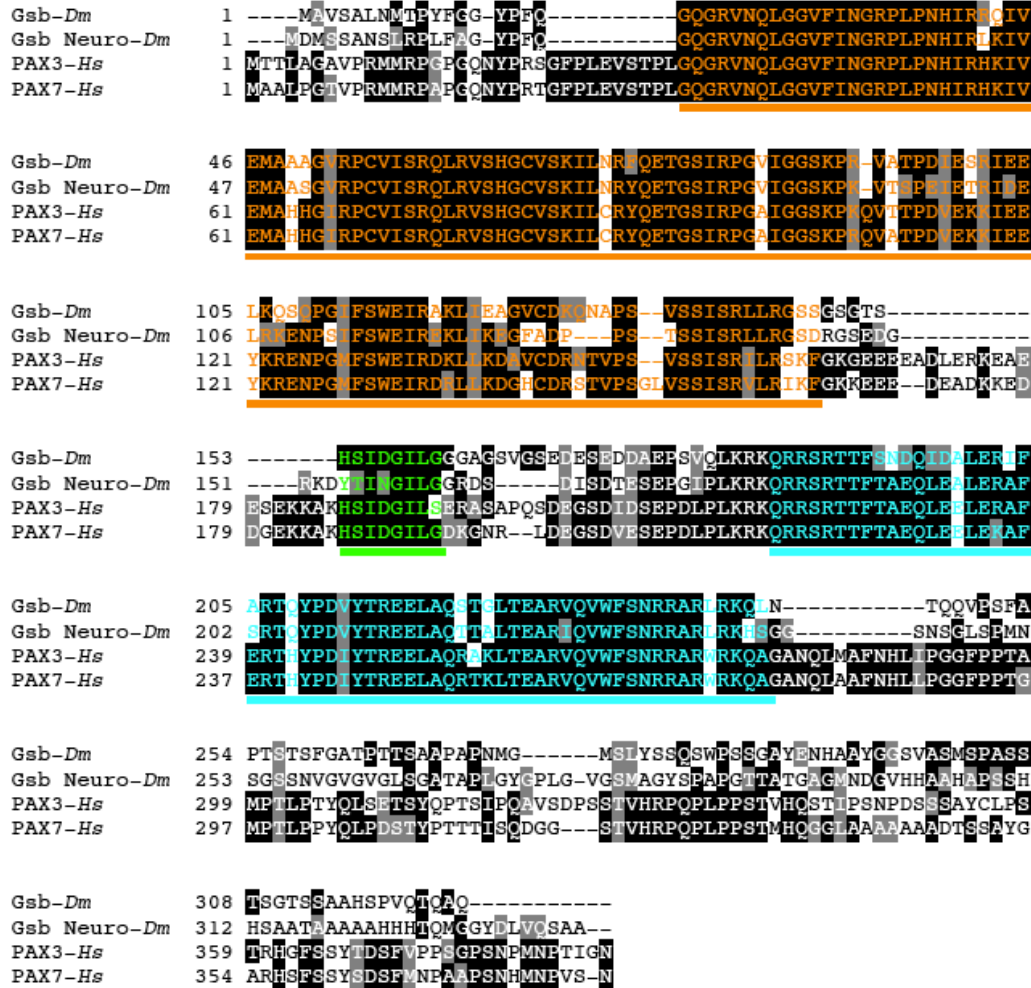


**Fig. 2.** PAX3/7 is conserved in *Drosophila*. The amino acid sequence alignment of human PAX3 and PAX7 and the *Drosophila* orthologs Gsb and Gsb-n are shown. Only the portion of the PAX3 and PAX7 proteins present in the PAX-FKHR fusion is displayed, and the Gsb and Gsb-n are abbreviated to show the equivalent portion to the PAX3/7 protein. The paired DNA binding domain is underlined in orange, the homeodomain is underlined in blue, and the octapeptide motif is underlined in green. *Dm*, *D. melanogaster*; *Hs*, *Homo sapien*.

A Myosin heavy chain-Gal4 (MHC-Gal4) driver was used to express either PAX3-FKHR or PAX7-FKHR in syncytial muscle fibers. Both PAX3-FKHR and PAX7-FKHR exhibited potent third instar larval and pupal lethality (though PAX7-FKHR is reproducibly more pathogenic, likely due to the fact that human PAX7 is slightly more identical in amino acid sequence than is PAX3). A UAS-GFP transgene that displays bright fluorescence and allows all syncytial body wall musculature to be observed through the larval cuticle was used to examine how PAX7-FKHR affects muscles *in vivo*. These PAX7-FKHR (MHC-Gal4, UAS-GFP, UAS-PAX7-FKHR) larvae demonstrated abnormal muscle morphology, exhibiting the absence of many individual syncytial muscle fibers with all muscle groups vulnerable, albeit in an indiscriminate pattern from animal to animal (Fig. 3). Additionally, the myofibers present appeared hypotrophic (Fig. 3h).

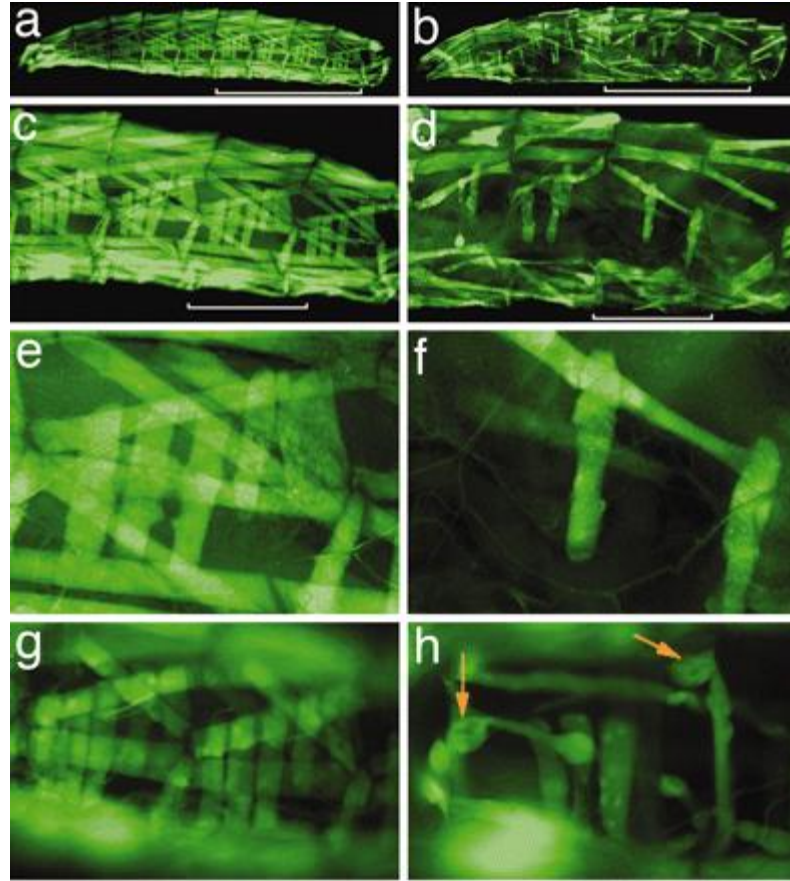


**Fig. 3.** PAX7-FKHR expression causes syncytial muscle fiber disarray in *Drosophila*. (a, c and e) Wild type. (b, d, and f) PAX7-FKHR. (a) Body wall musculature in a control MHC-Gal4, UAS-GFP third-instar larva. (b) Musculature in a MHC-Gal4, UAS-GFP, UAS-PAX7-FKHR third-instar larva. (c) Hemisegments of wild-type musculature. The four segments denoted by the white bar in *a* are shown. (d) Hemisegments of PAX7-FKHR musculature. The four segments denoted by the white bar in *b* are shown. (e) Abdominal hemisegment A6 in a wild-type animal. (f) Abdominal hemisegment A6 of a PAX7-FKHR larva displays abnormal musculature. (g) Hemisegments of a 2-day-old MHC-Gal4, UAS-GFP, UAS-PAX7-FKHR larvae. (h) The same PAX7-FKHR animal at 4 days of age highlighting dystrophic muscle tissue.

It was observed that first-instar larvae showed no clear expression of the UAS-GFP, suggesting that instead Gal4-driven expression of PAX7-FKHR accumulates in postnatal myofibers and specifically alters differentiated myofibers. In order to confirm this, a time-course study was conducted where the musculature of living PAX7-FKHR larvae were examined on sequential days of life and showed that they display

morphologically normal muscle up to two days of age. However, by day four, the musculature is clearly deteriorated and dysmorphic (Fig. 3h).

More detailed analysis of living animals expressing PAX7-FKRH revealed cellular-shaped tissue arising from the syncytial environment (Fig. 4b as compared with Fig. 4a), suggestive of new cells forming from differentiated myofibers. High-powered confocal microscopy of partially dissected larvae stained with DAPI to highlight nuclei demonstrated individual nucleated cells detaching from underlying myofibers (Fig. 4c and c') and separated mononuclear GFP-positive cells (Fig. 4d and e). This leads to the conclusion that PAX-FKHR can cause the development of individual myogenic mononuclear cells *de novo* from differentiated skeletal muscle. It was then observed that there was displaced GFP-positive tissue within internal soft tissue of the larvae including CNS, which does not normally contain elements of myogenic tissue (Fig. 5a'). No similar findings were seen in wild-type (MHC-Gal4, UAS-GFP) control animals. Confocal microscopy confirmed that the GFP-positive material contained nuclei which verified that PAX7-FKHR tissue circulates to and infiltrates non-muscle tissue compartments (Fig. 5c).

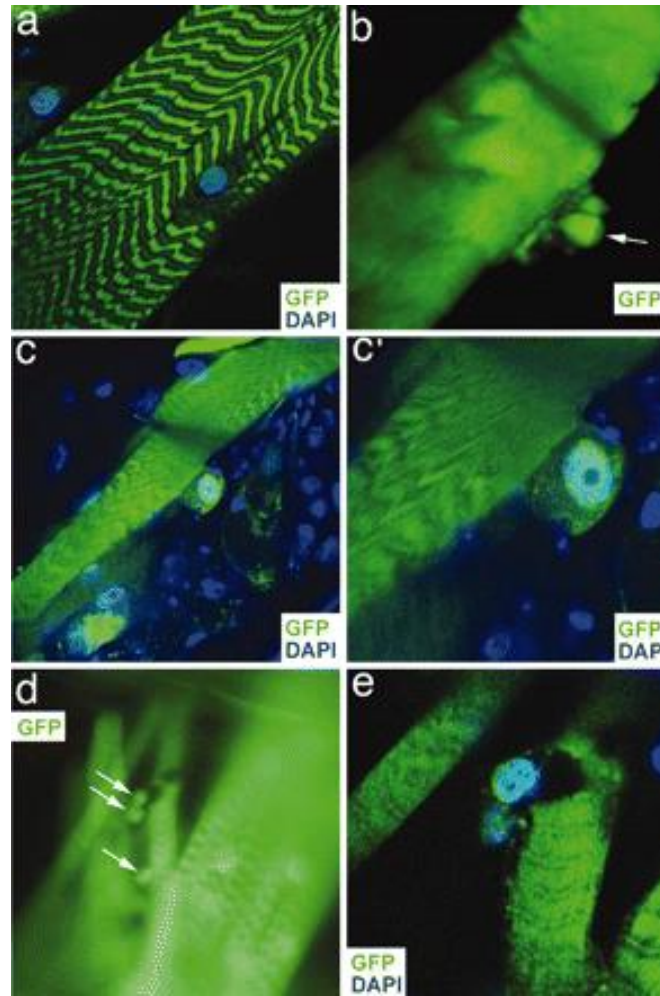


**Fig. 4.** PAX7-FKHR causes the development of mononuclear cells from the syncytial muscle environment. (a) Wild type. (b-e) PAX7-FKHR. (a) Myofiber of a wild-type control animal seen by confocal imaging. (b) A cell presumed to be arising *de novo* in syncytial muscle from a living PAX7-FKHR myofiber identified by the arrow. (c and c') A PAX7-FKHR expressing myofiber with a separating nucleated cell shown at two different magnifications. (d) A myofiber that has given rise to nucleated cells shows two cavities resulting from the newly separated cells (white arrows). It shows that the surrounding myofibers are intact, showing that this is not a disruption caused by dissection of the animal. (e) A confocal image of the same myofiber shown in d. (Magnifications: a,  $\times 60$ ; b,  $\times 252$ ; c and d,  $\times 63$ ; c',  $\times 152$ , e,  $\times 160$ .)

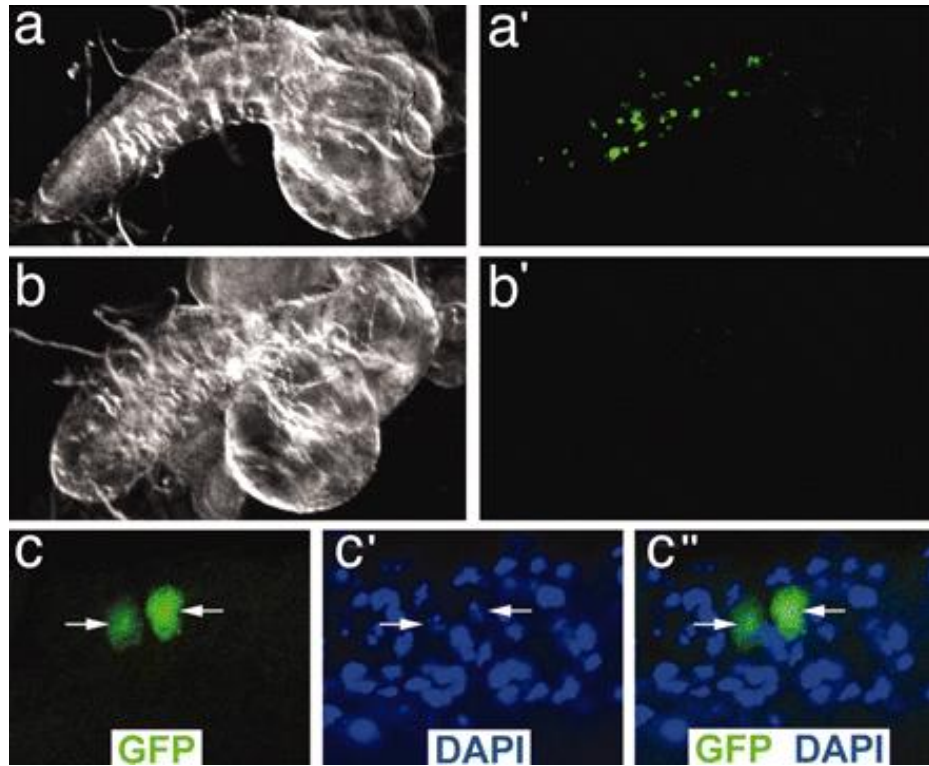


**Fig. 5.** PAX7-FKHR cells infiltrate the larval CNS. (a and a') A dark field (a) and GFP fluorescent (a') image of PAX7-FKHR CNS organ showing GFP-positive tissue. (b and b') A dark field (b) and GFP fluorescent (b') image of a wild-type CNS organ showing no GFP-positive signaling. (c-c'') Confocal images from a GFP-positive PAX7-FKHR larval CNS organ showing individual nuclei (white arrows) that correspond to GFP-positive cells.

Because PAX3-FKHR has been shown to be a weak oncogene in the transgenic alveolar rhabdomyosarcoma mouse model and required dysfunctional cell cycle checkpoints via mutations in Trp53 or Ink4a/ARF in order to obtain substantial quantities of animals displaying tumorigenesis, we tested whether *Drosophila* with dysfunctional cell cycle checkpoints would likewise express enhanced PAX7-FKHR activity. Tumor suppressor proteins such as p53 are not conserved in *Drosophila*, but constitutively active Ras has been associated with rhabdomyosarcomas and is known to disturb terminal differentiation of both human and fly muscle precursors. In the presence of both PAX7-



FKHR and Ras<sup>V12</sup>, a constitutively active *Ras* allele, the larval muscle patterns differed from both *wild-type* and *PAX7-FKHR* animals. They displayed a pattern of GFP fluorescence that was disordered and comparatively difficult to distinguish at low magnifications and even at high magnifications, the forms of many myofibers were indistinct (Fig. 6). Confocal microscopy of these fibers revealed mononuclear cells arising from the syncytial muscle environment with considerably higher incidence than with *PAX7-FKHR* alone (Fig. 6 d and e), and establishes gain-of-function *Ras* as an enhancer of the *PAX7-FKHR* phenotype.

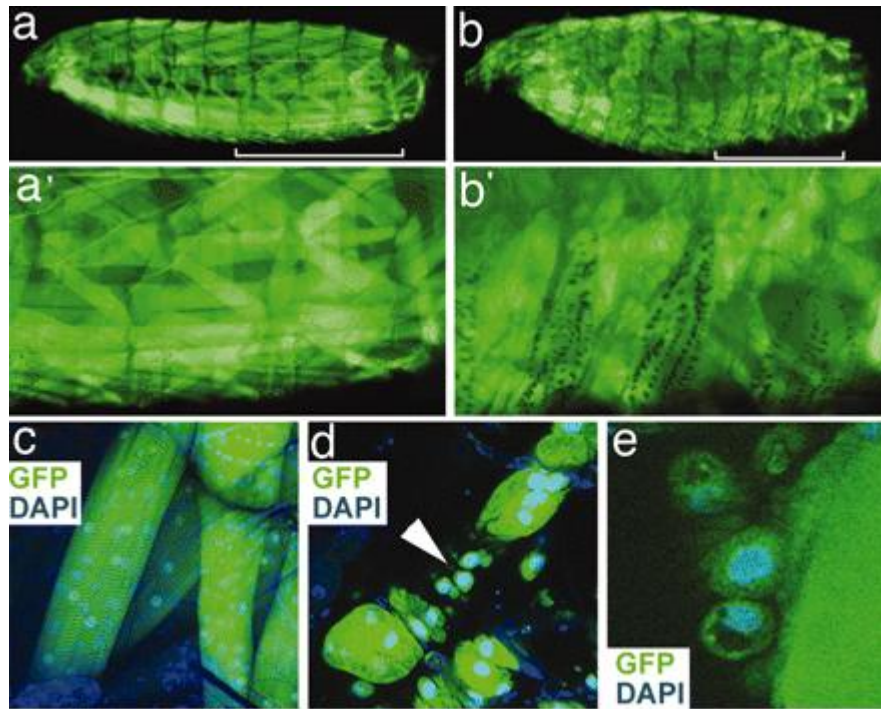


**Fig. 6.** Activated *Ras* enhances *PAX7-FKHR* muscular activity when co-expressed in syncytial muscle. (a and a') An MHC-Gal4, UAS-Ras<sup>V12</sup> larva. The three hemisegments indicated by the white bar are shown in a'. (b and b') An MHC-Gal4, UAS-Ras<sup>V12</sup> UAS-PAX7-FKHR larva. The three hemisegments indicated by the white bar are shown in b'. (c) Representative, stereotactically normal myofibers from an MHC-Gal4, UAS-Ras<sup>V12</sup> larva. (d and e) Abnormal myofibers from MHC-Gal4, UAS-Ras<sup>V12</sup> UAS-PAX7-FKHR larvae showing individual nucleated cells (arrowhead in d). Muscle tissue is highlighted by GFP expressed from the UAS-GFP transgene.

In order to further investigate the genetic interaction between Ras and PAX7-FKHR and to see if loss-of-function Ras would act as a suppressor of the PAX7-FKHR phenotype, we tested three lethal or semilethal loss-of-function Ras alleles ( $Ras^{E2f}$ ,  $Ras^{E1FB}$ , and  $Ras^{06677}$ ). The alleles dominantly suppressed the PAX7-FKHR phenotype to varying degrees. Suppression was confirmed in a blinded study with the most dominant suppressor,  $Ras^{E2f}$  (Fig. 7), such that 83 percent of the animals were rescued to viability versus the 15 percent of PAX7-FKHR larvae that survive to adulthood. This confirms that Ras is a clear genetic modifier of PAX7-FKHR.

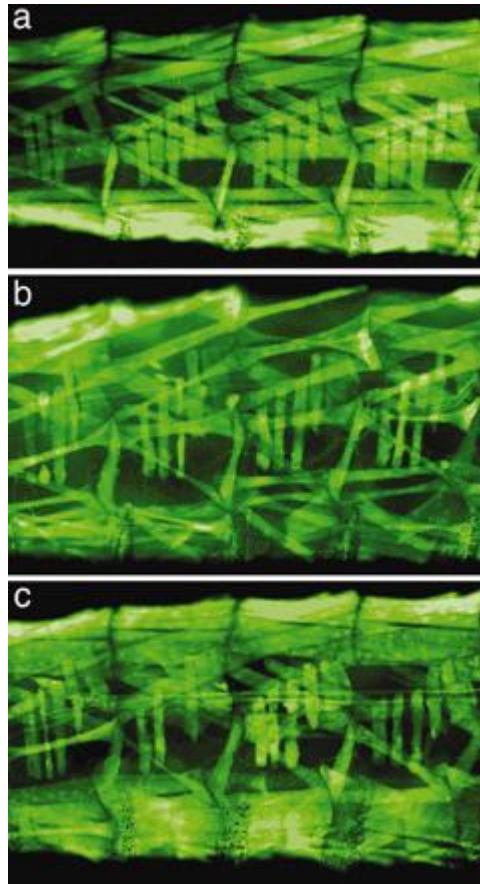


**Fig. 7.** A loss-of-function ras allele dominantly suppresses the PAX7-FKHR muscular phenotype. (a) Representative hemisegments of wild-type musculature. (b) Representative hemisegments of abnormal PAX7-FKHR musculature. (c) Representative hemisegments of PAX7-FKHR musculature with one loss-of-function  $ras^{E2f}$  allele. The number of intact myofibers is significantly increased in this genetic background.



## **DISCUSSION**

We have generated a new model using *Drosophila melanogaster* in order to explore the pathogenicity of PAX7-FKHR in alveolar rhabdomyosarcoma, which has demonstrated that PAX7-FKHR expression in differentiated muscle causes the development of individual nucleated cells from syncytial myofibers - cells that then spread to the CNS when liberated from myofiber attachment.

Although it has been the subject of much investigation, determining the tissue of origin for alveolar rhabdomyosarcoma has proved to be difficult. It has been previously hypothesized to be a muscle precursor cell or a stem-like cell because skeletal muscle is permanently postmitotic and syncytial, however transgenic expression of PAX3-FKHR in muscle precursor cells or muscle-specific satellite stem cells has not show evidence of tumorigenesis. Expression of PAX3-FKHR in terminally differentiating myofibers, however, causes tumorigenesis [3, 7]. Questions have persisted nonetheless, the possibility that the murine model was tumorigenic from an unidentified cell of origin because there was no data in cell culture or *in vivo* that PAX-FKHR induces individual cells to arise *de novo* from the syncytial muscle environment.

We expected that further investigation of the mouse model for subtle cellular changes would prove difficult because of the low percentage of PAX3-FKHR mice that actually grow tumors [3]. Instead we postulated that using a *Drosophila* model would offer a feasible model for this type of study due to the animal's susceptibility to rapid, sequential analysis of living muscle. Furthermore, fly muscle includes no known mechanism for repair, which prevents physiologic muscle regeneration from confounding

dysplastic phenotypes. Using our model system, we were able to provide evidence of cells arising *de novo* from myofibers, showing that PAX-FKHR can indeed trigger this process and that they form from differentiated muscle *in vivo*. This complements the data from the murine model and strongly argues that muscle tissue can function as the origin of rhabdomyosarcoma.

In order for alveolar rhabdomyosarcoma to stem from postmitotic muscle, the PAX-FKHR cells produced would need to re-enter the cell cycle in order to proliferate. This is supported by the fact that the PAX3-FKHR mouse models depend on loss of cell-cycle checkpoints in order to achieve meaningful levels of tumorigenesis and argues that alone PAX3-FKHR is not sufficient to cause cell-cycle reentry. We found no evidence of cell-cycle reentry in myofiber nuclei or the individual GFP-positive myogenic cells in either PAX7-FKHR or PAX7-FKHR, Ras<sup>V12</sup> flies after staining with phosphohistone H3 antibody. However, the gain-of-function and loss-of-function Ras studies intimate that Ras signaling does affect PAX7-FKHR-mediated dedifferentiation of muscle.

As the Ras enhancement and suppression studies show, the PAX7-FKHR *Drosophila* phenotypes are sensitive to genetic modification. This *PAX-FKHR* model is therefore well-adapted for unbiased genetic screens, which have yet to be utilized for PAX-FKHR and should reveal formerly unidentified gene targets and cofactors, thus suggesting new molecular mechanisms for PAX-FKHR rhabdomyosarcoma pathogenesis.

## CHAPTER THREE

### Molecular Mechanisms of PAX-FKHR Rhabdomyosarcoma

#### BACKGROUND

In order to identify new genetic interactors with PAX-FKHR, we conducted an unbiased forward genetic screen using the *PAX7-FKHR* *Drosophila* model. In addition to genetic screening, a microarray analysis was also performed comparing muscle tissue from *PAX7-FKHR Drosophila* and *wild-type Drosophila*. In the studies, the gene *antisocial (ants)*, was identified as a dominant suppressor of PAX-FKHR phenotypes and also as being misexpressed on the microarray. For these reasons, we chose to concentrate on *ants* as a likely PAX-FKHR responsive gene.

*Ants* is known to be a crucial player in the embryonic somatic muscle patterning and formation of syncytial fibers in *Drosophila*. It encodes a protein with multiple binding motifs that is required for attraction and interaction between founder cells and fusion-competent myoblasts. More specifically, *ants* is involved in myoblast fusion such that mature, multinucleated muscle fibers do not form in embryos with *ants* mutations. Instead they show collections of large quantities of unfused myosin-expressing myoblasts which retain the ability to differentiate and thus form mononuclear elongated myocytes. The expression of *ants* in the somatic mesoderm persists in *wild-type* flies until stage 15, which corresponds with termination of the myoblast fusion process [14].

*Ants* is the *Drosophila* ortholog of two mammalian genes, *mouse-ants1 (m-ants1)* and *mouse-ants2 (m-ants2)*, although no studies thus far have suggested that the vertebrate genes have a comparable function. Of both orthologues, *m-ants1* shows a

similar expression profile to that of *ants* in *Drosophila* embryo, seemingly critical for mesodermal development, indicating that *m-ants1* might be involved in vertebrate skeletal muscle formation. Like *ants*, *m-ants1* displays no expression in adult skeletal muscle [14].

## **METHODS**

### **Cell culture and Transient Transfections:**

C2C12 cells (ATCC) were grown in DMEM (Sigma-Aldrich) supplemented with 20% FBS (Atlas Biolabs). For Differentiation DMEM was supplemented with 2% horse serum (Sigma-Aldrich). Alveolar rhabdomyosarcoma cell line, RMS-13 was cultured in RPMI 1640 (Sigma-Aldrich) supplemented with 10% FBS. Transfections were carried out by electroporation. Cells were trypsinized after reaching 70% confluency and resuspended in Opti-MEM media and electroporated at 320 V, 960 microfarads with a Bio-Rad Gene Pulser II. Cells were differentiated after a day in growth media.

### **RNA extraction from paraffin embedded tumor samples and RT-PCR:**

Paraffin embedded tissue samples of ARMS were obtained from Children's medical center at Dallas. Tissue sections of 5  $\mu$ m thickness were made on a microtome and RNA was extracted following manufacture protocol for RecoverAll total nuclei acid isolation kit from Ambion. RT-PCR was performed using 100ng template RNA with Phusion RT-PCR kit from New England biolabs. Amplified products were confirmed by sequencing.

**Immunohistochemistry:**

Cells plated on four chamber slides after transfection with shTanc1 DNA (Open biosystems) were fixed with 4% paraformaldehyde and 0.1% Glutaraldehyde at room temperature for 5 min, permeablized and blocked with 0.1% Triton X-100 and 3% BSA in PBS for 15 min at room temperature. Antibodies used for detection were mouse MF-20 (1:400) (University of Iowa,Hybridoma bank) and Alexa-488 goat anti-mouse (1:5000) (Invitrogen). Cells were also stained with Rhodamine Phillodin (Invitrogen) for 10 min and mounted in vectaschield with DAPI. LSM510-meta confocal microscope (Zeiss, Thornwood, NY) was used for microscopy.

**Isolation of RNA from cells, cDNA synthesis and Real-time PCR:**

RNA was isolated from transfected cells following manufacture protocol for RNAqueous-Micro RNA extraction kit from Ambion. Reverse transcription was performed using 500ng of total RNA with Superscript III reverse transcriptase (Invitrogen). Quantitative real time PCR was performed using Brilliant II SYBR green QPCR master mix from Stratagene. Primers for Tanc1 were 5'ttggcgcctgcctggatgg 3' and 5' ccctcagtgcgctgtggacg 3', Tanc2 5'cctggatgagcagagacaca3' and 5' ttcgaagagtaggggcttca 3', and b-actin were 5' ccttctacaatgagctgcgtgtgg 3' and 5'acgaccagaggcatacagggacagc 3'.

## **RESULTS**

We relied upon mouse myoblast C2C12 cultured cells in to pursue uncovering the role of m-ants1 in mammalian myogenesis and myoblast fusion. These cells discontinue proliferation and begin to elongate and fuse to form multinucleated myotubes within four to six days of being placed in differentiation medium (Fig. 8 a and a'). Via reverse transcriptase-PCR (RT-PCR), C2C12 cells were found to express m-ants1. The following study using quantitative real-time PCR demonstrated a decreased expression of m-ants1 after C2C12 myoblast fusion and established that m-ants1 is indeed associated with myoblast cell fusion (Fig. 8c).

Subsequently, we used shRNA gene silencing to diminish endogenous m-ants1 expression in order to ascertain whether m-ants1 contributes to myoblast differentiation. The effectiveness of m-ants1 knockdown was verified via quantitative real-time PCR (Fig. 8d). This knockdown resulted in a cell culture predominantly composed of unfused mononuclear cells demonstrating that silencing m-ants1 results in impaired formation of myotubes and that m-ants1 plays a role in myoblast differentiation (Fig. 8 b and b').

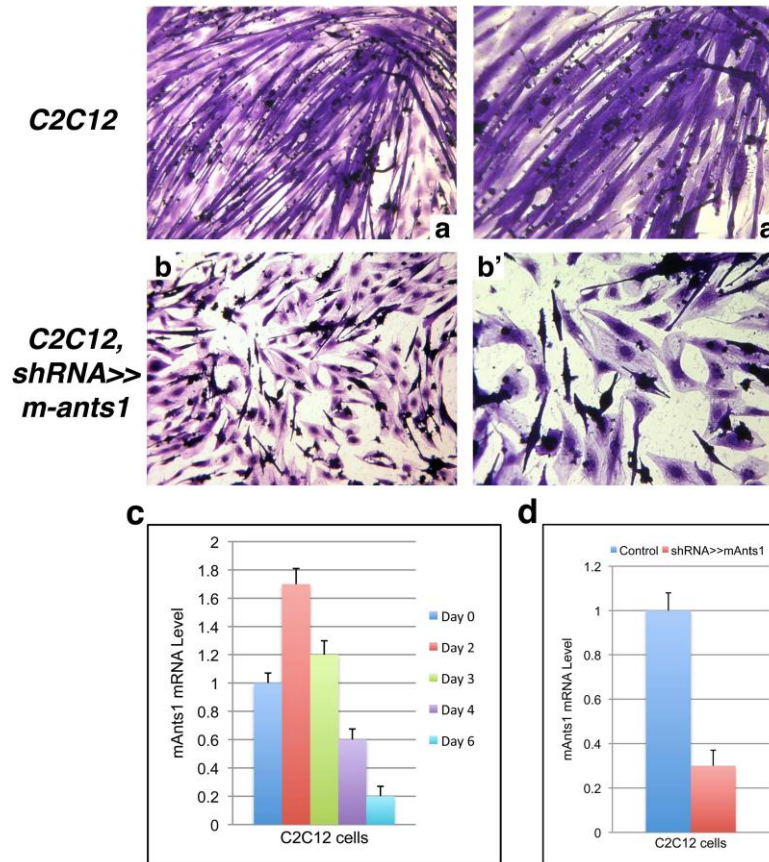


**Fig. 8.** Loss of m-ants1 severely blocks formation of myotubes. (a and a') C2C12 cells in differentiation medium fuse to form multinucleated myotubes. (b and b') m-ants1-silenced C2C12 cells in differentiation medium shows a population of unfused mononuclear cells. (c) Quantitative real-time PCR demonstrates decreased m-ants1 expression linked with cessation of myoblast cell differentiation and fusion in control C2C12 cells. (d) Quantitative real-time PCR demonstrates effective gene silencing of m-ants1 in m-ants1-silenced C2C12 cells.

There are several possible explanations for the mechanisms by which m-ants1 silencing might cause interruption of myotube formation. Loss of m-ants1 activity could potentially block the genetic myogenic program required for myoblast differentiation to myocytes and multinucleated syncytial myotubes. Alternatively, it may not disturb myocytes differentiation, but rather be involved in the machinery required for fusion of the myoblasts. We then performed immunohistochemical staining for muscle-specific Myosin Heavy Chain (MHC), which is a marker for late-to-terminally differentiated

muscle tissue, and showed that m-ants1 silenced C2C12 cells expressed similar levels of MHC as control C2C12 cells (Fig. 9). This suggests that myogenic differentiation does occur in m-ants1 silenced C2C12 cells, and that inability to complete cell-cell fusion is the underlying defect in m-ants1 deficient myoblasts.

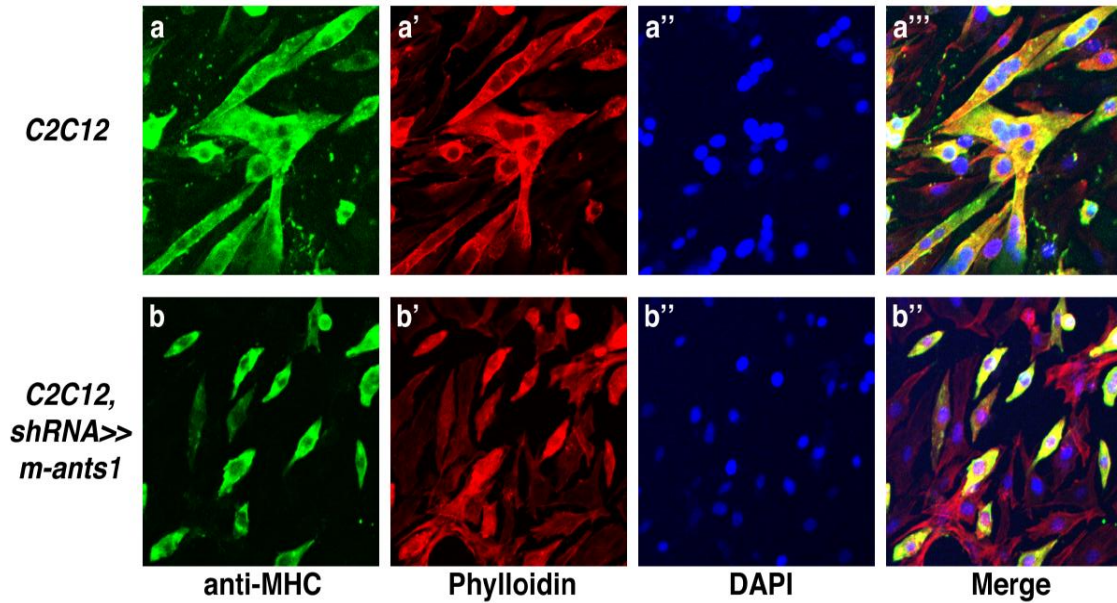


**Fig. 9.** M-ants1-silenced C2C12 myoblasts express comparable levels of MHC to control C2C12 myoblasts. (a, a', a'', and a''') Control C2C12 cells. (b, b', b'', and b''') m-ants1-silenced C2C12 cells. (a and b) Immunohistochemical staining for MHC. (a' and b') Immunohistochemical staining for phalloidin shows actin. (a'' and b'') Immunohistochemical staining with DAPI. (a''' and b''') Images from a, a' and a'' and b, b', and b'' merged to show a composite image.

Once we established that m-ants1 was in fact both present and functionally required in *wild-type* mammalian myoblasts, we then turned to the clinical issue of the role m-ants1 plays in rhabdomyosarcoma pathogenesis. Little is known about the pathogenesis of rhabdomyosarcoma, and the issue of whether defective fusion machinery is involved remains unexplored. We performed RT-PCR on mRNA extracted from human, paraffin-embedded PAX-FKHR rhabdomyosarcoma tumor tissue to confirm that



human ants1 (h-ants1) is expressed (Fig. 10a). We then repeated the RT-PCR using an established PAX-FKHR rhabdomyosarcoma cell line, RMS-13, and again detected the expression of h-ants1, suggesting that RMS-13 cell lines would be informative in studies testing the role of h-ants1 in RMS pathobiology.

Because our *Drosophila* PAX-FKHR data intimated that antisocial is a PAX-FKHR-responsive, up-regulated gene, we began testing the hypothesis that overexpression of h-ants1 in PAX-FKHR tumors might, at least in part, be responsible for or facilitate PAX-FKHR rhabdomyosarcoma pathogenesis. As before, we performed sh-RNA h-ants1 gene-silencing and verified effective knockdown via quantitative real-time PCR (Fig. 10b). Remarkably, the shRNA-treated IRMS-13 cells showed a phenotypically altered diffuse spindle-cell morphology which was suggestive of transition from primitive, round-cell myoblasts to elongating and differentiating spindle-cell myocytes (Fig. 10 d and d').

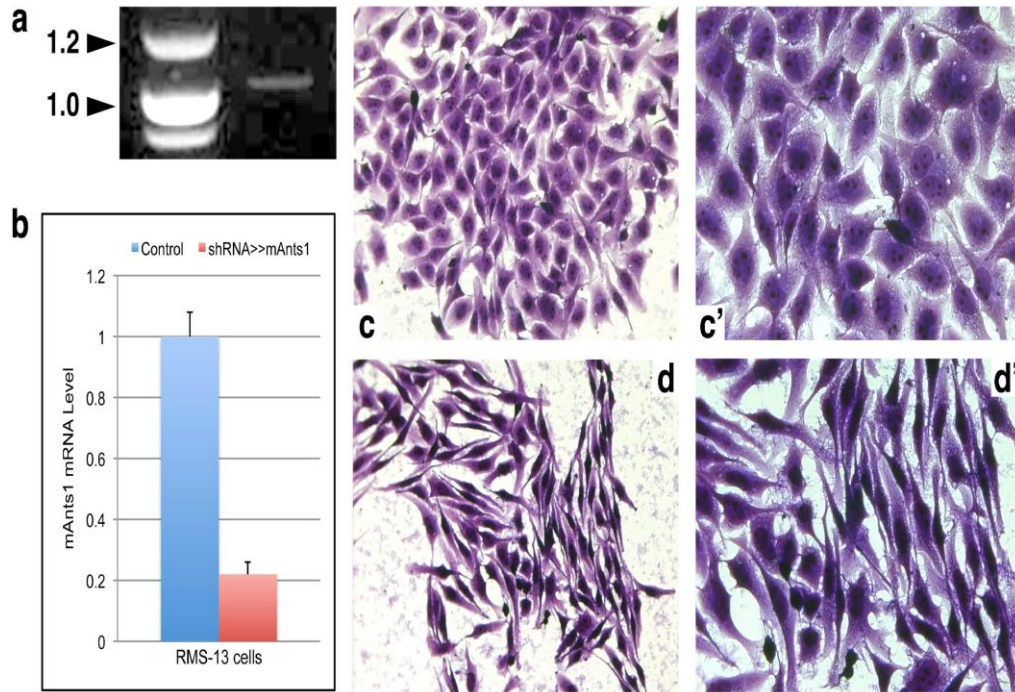


**Fig. 10.** Silencing m-ants1 in RMS-13 cells dramatically alters phenotype suggestive of transition from primitive myoblasts to differentiating myoblasts. (a) Image of RT-PCR confirms expression of h-ants1 in paraffin-embedded PAX-FKHR rhabdomyosarcoma tumor tissue. (b) Quantitative real-time PCR shows expression of h-ants1 in RMS-13 cell lines and effective h-ants1 silencing using sh-RNA. (c and c') Images of control RMS-13 cells show primitive myoblasts. (d and d') Images of h-ants1-silenced RMS-13 cells display elongated, spindle-cell myocytes.

We performed immunohistochemistry for MHC expression to check for rescue of myogenic differentiation. In contrast to control, mock-transfected RMS13 cells which are consistently negative for detectable MHC expression (Fig. 11a), MHC-positive RMS-13 cells were regularly observed and often demonstrated the spindled, myocyte cell morphology even though many other cells revealed no or low levels of detectable MHC (Fig. 11b). Even more informative was the easy identification of binucleated, “juvenile” myotubes and occasional multinucleated, “mature” myotubes which are highly suggestive of increased cell-cell fusion (Fig. 11 c and d). Based on these studies, we conclude that

reduction of h-ants1 expression in PAX-FKHR rhabdomyosarcoma cells partially rescues the developmental arrest, and thus the neoplastic phenotypes of rhabdomyosarcoma cells.

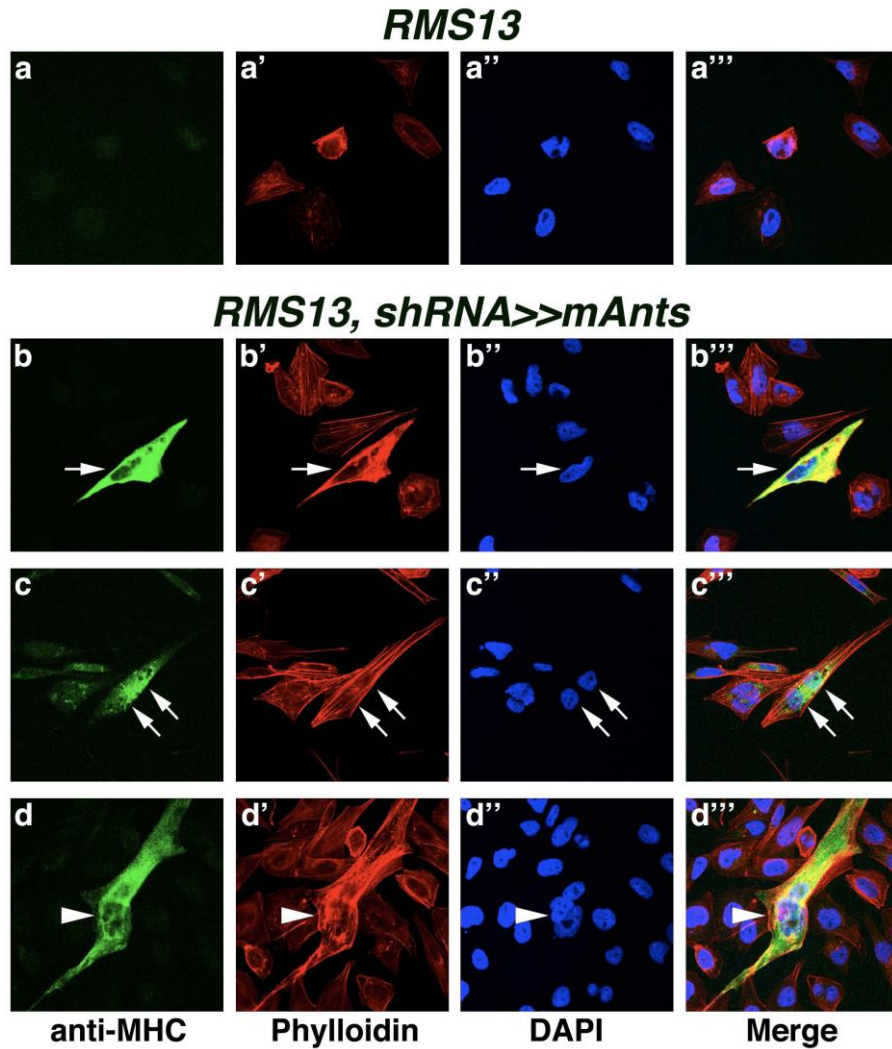


**Fig. 11.** Silencing h-ants1 expression in RMS-13 cells shows partial rescue of myogenic differentiation. (a, a', a'', and a''') Control RMS-13 cells. (b-b'', c-c'', and d-d'') h-ants1-silenced RMS-13 cells. (a) Immunohistochemical staining reveals RMS-13 cells are negative for detectable MHC expression. (a' and a'') Immunohistochemical staining shows expression of actin using phylloidin and nuclei using DAPI in RMS-13 cells. (a''') A composite of the stains in RMS-13 cells. (b) Immunohistochemical staining in h-ants1-silenced RMS-13 cells shows distinct expression of MHC. (b', b'', c', c'', d', and d'') Immunohistochemical staining shows expression of actin using phylloidin and nuclei using DAPI in h-ants1-silenced RMS-13 cells. (b'', c'', and d'') A composite of the stains in h-ants1-silenced RMS-13 cells. (c and d) Immunohistochemical staining in h-ants1-silenced RMS-13 cells demonstrates binucleated myotubes and the occasional mature, multinucleated myotubes.

## **DISCUSSION**

By taking advantage of invertebrate forward genetic screening and expression profiling, we identified the *Drosophila* *ants* gene as a PAX-FKHR responsive gene and downstream effector. After turning to mammalian myoblasts, we found that mammalian *ants* is crucial for the fusion of mouse myoblasts into multinucleated myotubes, although myogenic differentiation proceeds unrestricted in *ants*-lacking myoblasts. Finally, we revealed that decreasing *ants* expression in PAX-FKHR rhabdomyosarcoma cells at least partially rescues the myogenic differentiation arrest and fusion defects intrinsic to the RMS-13 cells.

Together, our findings argue for defective fusion machinery and failed cell-cell fusion as a new molecular mechanism underlying rhabdomyosarcoma pathogenesis. Due to the benefits of genetic screening, more is known about the molecular machinery necessary for myoblast fusion in *Drosophila*. Unfortunately, only a limited number of the *Drosophila* myoblast fusion genes, such as sticks and stones (ortholog to mammalian nephrin) and myoblast city (ortholog to mammalian DOC180) are known to participate in vertebrate myogenesis. We can now conclude that the antisocial intracellular adapter protein is likewise conserved.

Notably, in contrast to the myogenic transcription factors, myoblast fusion loci have not been investigated or implicated as rhabdomyosarcoma disease genes. We predicted and have shown, based on the extent of conservation of PAX biology and muscle development throughout evolution, that fusion defects are a mechanism underlying rhabdomyosarcoma pathogenesis. Although, surprisingly, we also observed

the restoration of myoblast fusion in PAX-FKHR rhabdomyosarcoma also corrects defects in myogenic differentiation, which was unexpected based on our C2C12 antisense silencing studies. It is noted however, that myoblast fusion defects in fly embryos do not cause blockage of myocytes differentiation. We propose that, at least in PAX-FKHR rhabdomyosarcoma cells, there is a checkpoint where cells must “sense” proper fusion or fusion potential before the down-regulation of myogenic factors, and therefore full genetic terminal differentiation, can occur. As a result, these studies suggest that a new therapeutic angle for rhabdomyosarcoma tumors may lie in targeting fusion defects.

Ultimately, we are confident that the genetic screening of the PAX-FKHR fly model is revealing new and informative PAX-FKHR cofactor and gene targets. Because little is known about the pathogenesis of rhabdomyosarcoma, particularly PAX-FKHR rhabdomyosarcoma, these genes present vital opportunities to make new mechanistic inferences about rhabdomyosarcoma pathogenesis. This information should present numerous points for complementary vertebrate biologic studies as well as new conceptual therapeutic approaches and targets which are selectively directed at these deadly pediatric tumors.

## BIBLIOGRAPHY

1. **Arndt CA, Crist WM** 1999 Common musculoskeletal tumors of childhood and adolescence. *New England Journal of Medicine* 341:342-52
2. **De Giovanni C, Landuzzi L, et al** 2009 Molecular and cellular biology of rhabdomyosarcoma. *Future Oncology* 5:1449-75
3. **Keller C, Arenkiel BR, et al** 2004 Alveolar rhabdomyosarcomas in conditional pax3:Fkhr mice: Cooperativity of ink4a/arf and trp53 loss of function. *Genes and Development* 18:2614-26
4. **Nishijo K, Chen QR, et al** 2009 Credentialing a preclinical mouse model of alveolar rhabdomyosarcoma. *Cancer Research* 69:2902-11
5. **Pappo AS, Shapiro DN, et al** 1997 Rhabdomyosarcoma: Biology and treatment. *Pediatric Clinics of North America* 44:953-72
6. **Galindo RL, Allport JA, et al** 2006 A drosophila model of the rhabdomyosarcoma initiator pax7-fkhr. *Proceedings of the National Academy of Sciences of the United States of America* 103:13439-44
7. **Keller C, Hansen MS, et al** 2004 Pax3:Fkhr interferes with embryonic pax3 and pax7 function: Implications for alveolar rhabdomyosarcoma cell of origin. *Genes and Development* 18:2608-13
8. **Jostes B, Walther C, et al** 1990 The murine paired box gene, pax7, is expressed specifically during the development of the nervous and muscular system. *Mechanisms of Development* 33:27-37

9. **Greaves MF, Wiemels J** 2003 Origins of chromosome translocations in childhood leukaemia. *Nature Review Cancer* 3:639-49
10. **Felix CA, Kappel CC, et al** 1992 Frequency and diversity of p53 mutations in childhood rhabdomyosarcoma. *Cancer Research* 52:2243-7
11. **Brand AH, Perrimon N** 1993 Targeted gene expression as a means of altering cell fates and generating dominant phenotypes. *Development* 118:401-15
12. **Gutjahr T, Patel NH, et al** 1993 Analysis of the gooseberry locus in drosophila embryos: Gooseberry determines the cuticular pattern and activates gooseberry neuro. *Development* 118:21-31
13. **Xue L, Li X, et al** 2001 Multiple protein functions of paired in drosophila development and their conservation in the gooseberry and pax3 homologs. *Development* 128:395-405
14. **Chen EH, Olson EN** 2001 Antisocial, an intracellular adaptor protein, is required for myoblast fusion in drosophila. *Developmental Cell* 1:705-15

# Vitae

## Education

**University of Texas at Austin**, Austin, TX, 8/04-05/07

Bachelor of Arts – May 2007

Magna Cum Laude

Major: Biology

GPA: 3.97/4.0

**Lone Star College**, Spring, TX (Summer School: 6/05-7/05)

GPA: 4.0/4.0

## Work Experience

**NIH T-35 Grant Research Fellow**, University of Texas Southwestern Medical Center at Dallas,  
Department of Pathology, Dallas, TX, 06/09-08/09

- Research on mechanisms of rhabdomyosarcoma and genes thought to be responsible
- Perform PCR, cloning, restriction digestion, gel electrophoresis and other molecular biology techniques
- Attend regular lecture given by experts in the fields of cancer and molecular biology

**Research Fellow**, University of Texas Southwestern Medical Center at Dallas,  
Department of Dermatology, Dallas, TX, 06/08-08/08

- Researched the effectiveness of novel hyaluronidase probe in melanoma cells
- Maintained B16-F10 cell line and performed cell culture
- Performed FACS analysis

**Medical Study Abroad Program**, University of Texas at Austin,  
Universidad de Guadalajara, Guadalajara, Mexico, 7/06-12/06

- Rounded with medical students at Hospital Civil Viejo in 4 week long rotations
- Attended medical school classes at Universidad de Guadalajara
- Participated in an intensive 6 week Spanish class

### Clinic Volunteer

El Buen Samaritano Clinic, Austin, TX, 08/05-12/07

- Managed patient records and performed basic office functions
- Took vital signs and brief patient history
- Shadowed staff of volunteer nurses and physicians

## Honors & Awards

### University of Texas Southwestern Medical Center at Dallas

2010	SSPR/APA trainee travel award Southern Soc. for Pediatric Research
2009	NIH T-35 grant for medical student summer research
2008	SUMR grant for medical student summer research

### University of Texas at Austin

2007	Magna Cum Laude
2007	Phi Beta Kappa
2005-2007	University Distinguished Scholar



## **Publications and Presentations**

Edelman LA, Mummert ME. 2009. Detection of Hyaluronidase Activity In Vitro Using FRET-HA. *47th Medical Student Research Forum Booklet*. 13.

Edelman LA, Galindo RL. 2010. Molecular Dissection of Rhabdomyosarcoma Tumorigenesis. *48<sup>th</sup> Medical Student Research Forum Booklet*. 6.

Edelman LA, Avirneni-Vadlamudi U, Tran LT, Galindo, RL. 2010. Molecular Dissection of Rhabdomyosarcoma Tumorigenesis. *Journal of Investigative Medicine*. 58:453.

Lauren Edelman, Oral Presentation, **Southern Regional Meeting**, New Orleans, Louisiana, 2010.

## **Memberships & Associations**

2008-2011	Pathology Interest Group, Secretary
2008-2011	American Medical Association
2004-2007	Gamma Beta Phi Honor Society
2004-2007	Alpha Phi Omega National Boy Scouts of America Fraternity